Heliyon 10 (2024) e35341

Contents lists available at ScienceDirect

Heliyon

journal homepage: www.cell.com/heliyon

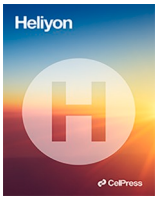

Research article

Tirofiban prevents the effects of SARS-CoV-2 spike protein on macrophage activation and endothelial cell death

Laura Marrone [a], Simona Romano [a], Michele Albanese [b,c], Salvatore Giordano [d], Alberto Morello [b,c], Michele Cimmino [b,c], Valeria Di Giacomo [a], Chiara Malasomma [a], Maria Fiammetta Romano [a,*], Nicola Corcione [b,c]

[a] Department of Molecular Medicine and Medical Biotechnology, University of Naples Federico II, Naples, Italy
[b] Cardiovascular Interventions Unit, Pineta Grande Hospital, Castel Volturno, Italy
[c] Hemodynamics Unit, Santa Lucia Hospital, San Giuseppe Vesuviano, Italy
[d] Division of Cardiology, Department of Medical and Surgical Sciences, "Magna Graecia" University, Catanzaro, Italy

ARTICLE INFO

Keywords:
SARS-CoV-2
Spike
Macrophage
β3 integrin

ABSTRACT

SARS-CoV-2 viral-derived particles have been proposed to have a causal role in tissue inflammation. Macrophage is the culprit cell in the pathogenesis of destructive inflammatory response to the SARS-CoV-2 virus. We investigated whether the spike protein might play a role in perturbing the physiological process of resolution of inflammation. Using an in vitro model of M2 polarized macrophages, we found that recombinant spike protein produced typical M1 morphological features in these alternative differentiated cells. In the presence of spike, M2-macrophages lose their elongated morphology, become rounded and acquire a strong capability to stimulate lymphocyte activation and proliferation. Moreover, in M2 macrophages, spike activated the signal transducer and activator-1 (STAT1) the pivotal mediator of pro-inflammatory macrophages. We observed STAT1 activation also in endothelial cells cultured with recombinant spike, accompanied by Bax upregulation and cell death. Blockade of beta3 integrin with the RGD mimetic tirofiban reverted the spike-induced costimulatory effects on M2 macrophages. Also, tirofiban counteracted STAT1 and Bax activation in endothelial cells cultured with spike and reduced endothelial cell death. In conclusion, we found that some proinflammatory effects of the spike protein can involve the integrin pathway and provide elements supporting use of RGD mimetics against SARS-Cov-2.

1. Introduction

SARS-CoV-2 is a viral strain belonging to the coronavirus subfamily, responsible for severe acute respiratory syndrome (SARS). The infection causes inflammation of the endothelium, leading to vascular pathologies, particularly thrombosis, and is complicated by interstitial pneumonia and severe respiratory failure. The entry of the virus into the host cell occurs through the interaction of the viral structural protein spike and its receptor angiotensin-converting enzyme 2 (ACE2) [1]. ACE2 provides an endogenous counter-regulation mechanism within the renin-angiotensin system balancing the vasoconstrictor and hypertensive effects of angiotensin II [2]. Integrin β3 is another recognition structure for SARS-CoV-2 [3,4] due to the presence of an RGD (Arg-Gly-Asp)

* Corresponding author.
E-mail address: mariafiammetta.romano@unina.it (M.F. Romano).

https://doi.org/10.1016/j.heliyon.2024.e35341
Received 22 August 2023; Received in revised form 25 July 2024; Accepted 26 July 2024
Available online 31 July 2024

integrin-binding motif in the receptor binding domain of spike protein [5].

Although SARS-CoV-2 infection may be asymptomatic or cause only mild symptoms in most cases, excessive inflammatory response to the virus, resulting in significant destructive consequences for the host, occurs in nearly 10–20 % of the patients [6]. Macrophage is the culprit cell in the pathogenesis of such an unfavorable condition, producing the so-called "cytokine storm" that represents the leading cause of death [7].

Macrophages are innate immune cells that first encounter pathogens [8]. Following tissue injury induced by an infectious agent, they differentiate into an M1 pro-inflammatory phenotype that triggers an adaptive immune response promoting the lymphocyte-mediated killing of both pathogen and infected cells [8–10]. Thanks to their plasticity, once the pathogen is eliminated, the macrophages progressively develop a functional anti-inflammatory or M2 phenotype, initiating repair and recovery and driving the resolution of tissue damage [11–14]. When this physiological mechanism of M1 to M2 switching that restores tissue homeostasis is disrupted, persistent inflammation prolongs and amplifies disease, and macrophages become major contributors to tissue destruction [15].

As SARS-CoV-2 viral-derived particles have been proposed to have a causal role in tissue inflammation [16], we hypothesized that the spike protein might contrast the physiological process of resolution of inflammation. Using an in vitro model of M2 polarization, we investigated whether recombinant protein could reprogram the M2-to-M1 phenotype.

2. Materials and methods

2.1. Peripheral blood mononuclear cells (PBMCs) isolation

PBMCs were isolated by differential centrifugation through a Ficoll–Hypaque density gradient (Histopaque-1077, Sigma-Aldrich, St. Louis, MO, USA). Cells were washed and resuspended in 10 % heat-inactivated fetal bovine serum (FBS)/Roswell Park Memorial Institute (RPMI) 1640 medium (Biowest, Nuaillè, France). After the count, PBMCs were processed for further analysis.

2.2. Cell culture and reagents

Isolated PBMCs and human monocytic THP-1 cells were cultured in RPMI 1640 supplemented with 10 % heat-inactivated FBS, 200 mM glutamine (Lonza; Basel, Switzerland), and 100 U/ml penicillin-streptomycin (Lonza) at 37 °C in a 5 % CO_2 humidified atmosphere. ECV-304 were cultured in Dulbecco's Modified Eagle's Medium (DMEM) (Corning, Glendale, Arizona, USA) supplemented with 10 % heat-inactivated FBS, 200 mM glutamine, and 100 U/ml penicillin-streptomycin. HUVEC were purchased from Lonza and cultured in an endothelial cell growth medium supplemented with growth factors and serum (Lonza).

Six-well plates were precoated with 100 ng/ml in 1X Phosphate buffered saline (PBS) spike recombinant proteins (full-length wt and Δ SARS-CoV-2 spike proteins) by an overnight incubation at 4 °C. Bovine serum albumin (BSA) (Sigma-Aldrich) was used at the same coating dose of 100 ng/ml as negative control. Full-length spike wt and Δ SARS-CoV-2 were purchased by Bio-Techne Corporation, Minneapolis, MN, USA. After incubation, wells were washed with 1X PBS, and PBMCs- or THP1- derived macrophages (7×10^5 cells) were seeded onto each well. Tirofiban hydrochloride monohydrate (Aggrastat) was from Correvio (London, UK). The monoclonal antibody abciximab (Reopro) was from Eli Lilly and Company Limited (Basingstoke, NL). Tirofiban and abcximab were added to macrophage cell suspension before seeding on spike-coated plates. The doses used for tirofiban (1 μg/ml) and abciximab (10 μg/ml) were in accordance with a previous paper [17].

2.3. Macrophage polarization and counts

Polarization of primary macrophages was performed according to Yu et al. [18]. Polarization of the THP-1 monocytic cell line was performed according to Baxter et al. [19]. Briefly, PBMCs were stimulated for 6 days with M-CSF (Immunotools, Friesoythe, Germany) used at a final concentration of 50 ng/ml and then polarized into M1 macrophages with 100 ng/ml IFNγ (Immunotools) and 100 ng/ml LPS (Sigma-Aldrich) or M2 macrophages with 50 ng/ml IL-4 (Immunotools) for 48 h. THP-1 monocytes are differentiated into macrophages by a 72 h incubation with 100 ng/ml phorbol 12-myristate 13-acetate (PMA, Sigma-Aldrich) followed by a 24 h incubation in RPMI medium. THP-1-derived macrophages were then polarized in M1 macrophages through stimulation with 20 ng/ml IFNγ (Immunotools) and 100 ng/ml LPS (Sigma-Aldrich) or M2 macrophages with 20 ng/ml IL-4 (Immunotools), for further 48 h. Macrophages on the monolayer were counted, at least, in three different areas, and classified in M1 (roundly/elongated) or M2 (stretched/dendritic) based on the mere observation of their morphologic aspects using an inverted microscope (DMI4000; Leica Microsystems, Heidelberg, Germany) at 20× magnification with Leica Application Suite Advanced Fluorescence (LASAF) software (Leica Microsystems). The number of rounded (or slightly elongated cells) (M1-like) and the number of stretched/dendritic cells (M2-like) were counted and the cell count was represented as rounded/dendritic ratio. Dendritic cell morphology was defined according to the number of protrusions of each cell: numbers of protrusions greater than 2 were associated with dendritic forms (M2-like). Measurements were performed in 3–6 different fields (>50 cells) per experimental point using ImageJ 1.52p software. Dead cells were assessed by propidium iodide (PI, Sigma-Aldrich) staining (5 μg/ml in PBS) of the macrophage monolayer. The number of PI positive cells was counted on the number of total cells and represented as percentage %. Images were acquired at 10× magnification on a confocal microscope (Thunder Imager 3D cell culture microscope) with a Leica Thunder Imaging System (Leica Microsystems Wetzlar, Germany) and at least 100 cells per field were counted.

2.4. T cell activation and coculture

PBMCs activation was performed by stimulating the cells for 12 h in the presence 10 μg/ml anti-CD3 monoclonal antibody (Functional Grade, eBioscience, Thermo Fisher Scientific, Waltham, MA, USA) (0.2 beads per cell). Cells were washed three times with a 10 % FBS-culture medium, and then cocultured with autologous M1 or M2 macrophages in a spike precoated well. PBMCs were harvested after 72 h of coculture.

2.5. Flow cytometry analysis

BD-Pharmigen Fc block (2.5 μg/10^6 cells) was used to minimize the non-specific binding of immunoglobulins to Fc receptors, before immuno-staining [20]. Cells were resuspended at the concentration of 2×10^6/ml. Five–10 μl of antibody recognizing the typical cluster differentiation (CD) were added to 50 μl of cell suspension, and incubated for 30 min in the dark at 4 °C. The following antibodies were used: anti-CD80-APC (MEM-233 clone; Immunotools, Friesoythe, Germany), or anti-Hu CD80-BV650 (L307.4 clone, BD Horizon™, East Rutherford, New Jersey), Anti-Hu HLA-DR-PE (L243 clone; Invitrogen-Thermo Fisher Scientific), anti-Hu CD206-BV480 (19.2 clone, BD OptiBuild™), anti-CD4-PerCP (VIT4 clone, Miltenyi Biotec, Biotec, Bergisch Gladbach, Germany) or anti-CD4-FITC (VIT4 clone, Miltenyi Biotec). Anti-Hu ACE-2 PE (AC18F clone, Novus Biological, Abingdon, UK). The expression of β3 was measured using the monoclonal antibody abciximab (7E3) conjugated with 5-carboxyfluorescein (FAM). 7E3 conjugation was performed using an AnaTagTM 5-FAM Protein Labeling Kit (AnaSpec, Fremont, CA, USA) [17]. For intracellular staining, 200 μl of a fixation/permeabilization buffer (BD-Pharmingen Cytofix/Cytoperm Kit, San Jose, CA, USA) was added to each tube and incubated for 20 min in the dark at 4 °C. Then, the cells were incubated with the following antibodies: Anti-Hu Ki67 APC (SolA15 clone; eBioscience, Thermo Fisher Scientific), anti-IL10-PE (JES3-9D7 clone, eBioscience), anti-Hu IFNγ -PE (B27 clone, Immunotools). For intranuclear staining, 200 μl of Transcription Factor Staining Buffer Set (eBioscience, Thermo Fisher Scientific) was added to each tube and incubated for 20 min in the dark at 4 °C. After nuclear permeabilization, the cells were incubated with anti-Foxp3-PE (PCH101 clone, eBioscience, Thermo Fisher Scientific). For each staining, a relative Ig isotype-conjugated antibody was used as a control of non-specific binding. Gating strategy and subset counts were performed as previously described [20]. Analysis of cell death was performed by propidium iodide and annexin V staining. Briefly, 1x10 cells were harvested after a 24 h culture and resuspended in 100 μl of binding buffer (10 mM Hepes/NaOH pH 7.5, 140 mM NaCl, 2.5 mM CaCl2) containing 5 μl of annexin V-FITC (Pharmigen/Becton Dickinson, San Diego, CA) and 10 μl of a 50 μg/ml PI stock (Sigma-Aldrich) for 15 min at room temperature, in the dark. Then 400 μl of the same buffer was added to each sample and cells were analyzed with the flow cytometer. Samples were analyzed using a BD AccuriTM C6 Cytometer (Becton, Dickinson and Company BD; Bergen County, NJ, USA). The flow cytometry data were analyzed by using the FlowJo software or the C6 Accurì software.

2.6. qPCR

Total RNA was isolated from cells using Trizol reagent (Invitrogen-Thermo Fisher Scientific) according to the manufacturer protocol. cDNA was synthesized by random hexamers with iScript cDNA synthesis kits (Bio-Rad, Hercules, CA, USA), according to the protocols supplied by Bio-Rad. After digestion with DNAse RNAse-free, 2 μg of total RNA in 20 μl was used in each reaction. qRT-PCR was performed using the iQSYBR Green Supermix (Bio-Rad) and Bio-Rad CFX96 real-time PCR detection system, according to the protocols supplied by Bio-Rad. The primers were designed with Primer 3 program; sequences are reported below. All RTqPCRs were performed in duplicate, with 50–100 ng ss-cDNA used in each 15-μl reaction. SDHA, RPS18 or HPRT mRNA were used to normalize the mRNA concentrations. Gene expression was quantified as previously described [21].

Oligo sequences are reported:

h- IL10 -Fw: 5′-GGCACCCAGTCTGAGAACAG-3′;
h- IL10-Rev: 5′-TGGCAACCCAGGTAACCCTTA-3′;
h-IL4 - Fw: 5′-TTGCTGCCTCCAAGAACACA-3’;
h-IL4-Rev: 5′-TCCAACGTACTCTGGTTGGC -3′
h-SDHA-Fw 5′-TGGGAACAAGAGGGCATCTG-3’;
h-SDHA-Rev 5′-CCACCACTGCATCAAATTCATG-3′;
h-RPS18-Fw 5′- CGATGCGGCGGCGTTATTC-3′;
h-RPS18-Rev-5′- TCTGTCAATCCTGTCCGTGTCC-3′.
hIL17-Fw: 5′-CCAAAAGCCTGAGAGTTGCC-3’;
hIL17-Rev: 5′-TTGATGCAGCCCAAGTTCCT-3’;
h-HPRT- Fw-5′-TGACACTGGCAAAACAATGCA-3’;
h-HPRT -Rev-5′-GGTCCTTTTCACCAGCAAGCT-3’;
h-IL-6-Fw: 5′-GGTACATCCTCGACGGCATCT-3’;
h-IL-6-Rev:5′-GTGCCTCTTTGCTGCTTTCAC-3;
h-ARG1-Fw: 5′-GGCTGGTCTGCTTGAGAAAC-3′;
h-ARG1-Rev: 5′-CTTTTCCCACAGACCTTGGA-3′;
h-iNOS-Fw: 5′-CAGCGGGATGACTTTCCAA-3′;
h-iNOS-Rev: 5′-AGGCAAGATTTGGACCTGCA-3′;

2.7. Western blot

Whole-cell lysates were prepared from the cells as previously described [22] and assayed by immunoblot. Protein concentration was determined using the Bradford protein assay (Bio-Rad), measuring absorbance at 595 nm. Cell lysates were equalized for total proteins, and the final volume was leveled with water and Laemmli sample buffer (LB). Samples were denatured for 5 min at 95 °C, then loaded in 8/10 % T SDS-PAGE and transferred into a methanol-activated PVDF membrane (Immobilon-P; Millipore, Sigma-Aldrich). The membranes were incubated with the corresponding primary antibody at 4 °C overnight. Primary antibodies against the following proteins were diluted as follows: anti-phospho-STAT1 (Tyr 701) (GTX50118, Genetex; Irvine, CA, USA) (1:1000), anti-STAT1 (sc464, Santa Cruz Biotechnology; Santa Cruz, CA, USA) (1:500), anti-Bax (B9, sc-7480, Santa Cruz Biotechnology) (1:500), Anti-β-Actin, (15G5A11/E2, Invitrogen-Thermo Fisher Scientific) (1:5000), γ-tubulin (T9026, Sigma-Aldrich) (1:5000). After washes, membranes were incubated with secondary antibodies for 1 h, at room temperature. Anti-mouse and anti-rabbit secondary antibodies HRP-conjugated were purchased from ImmunoReagents (Raleigh, NC, USA) and were diluted at 1:5000. The protein bands were visualized with a chemiluminescence detection system (Western Blotting Luminol Reagent, Santa Cruz Biotechnology). Quantification of bands was obtained by densitometry analysis using ImageJ 1.42q for Macintosh; integrated optical densities of each analyzed protein were normalized to a relative housekeeping gene, and values were expressed as fold change of protein levels in the different samples in comparison with a control sample whose expression was arbitrarily indicated equal to 1.

2.8. Statistical analysis

Mann-Whitney and Student's t-test assessed differences in means of values between two groups, using Prism GraphPad 7.0a for

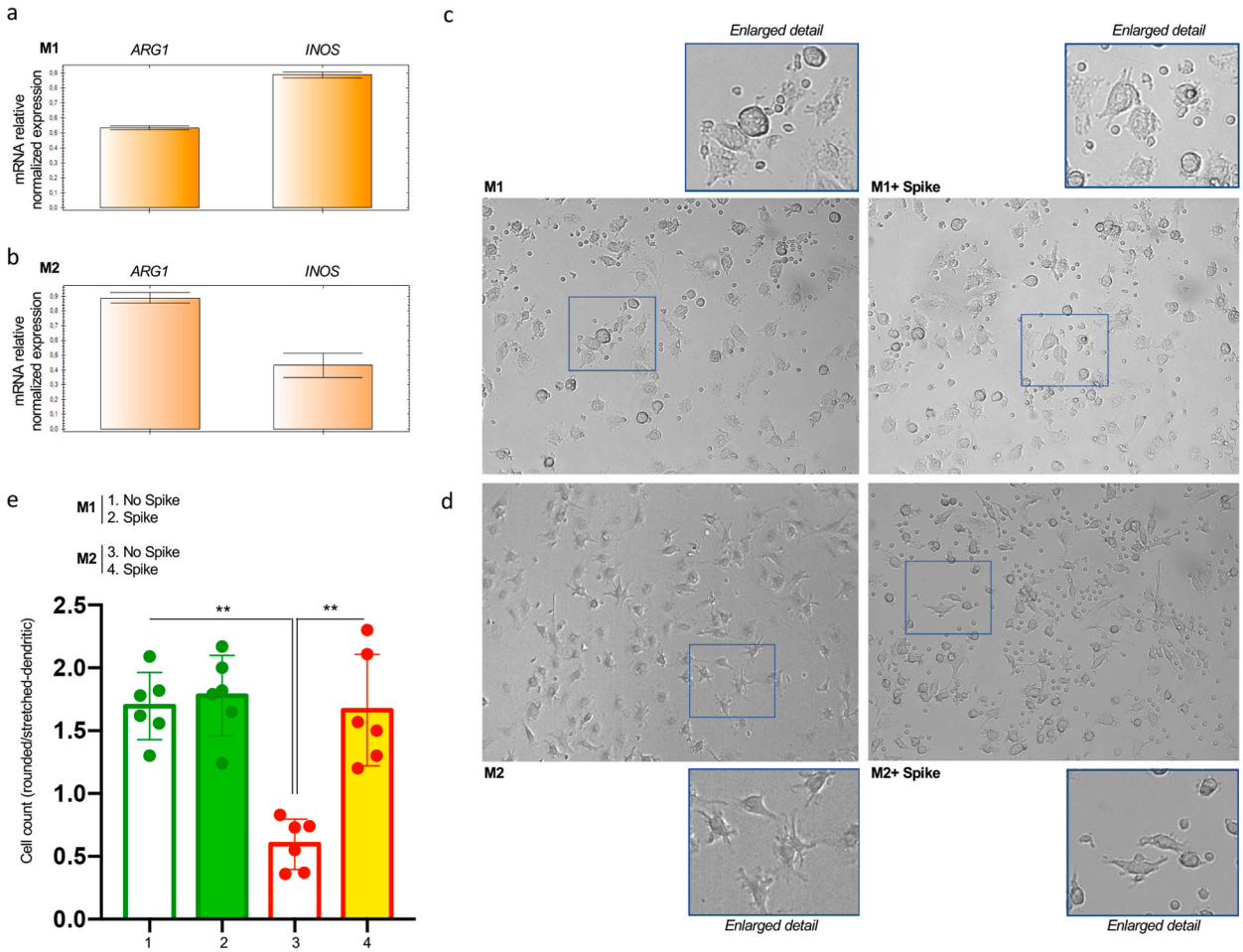

Fig. 1. Spike induces M2 to M1 morphologic switch (a, b) RT-qPCR analysis of mRNA levels of ARG1 and iNOS in PBMCs-derived M1 (a) and M2 (b) macrophages. Values are expressed as mRNA relative normalized expression. (c, d) Representative images acquired under an inverted microscope (Leica DMI4000) at 20 × magnification showing morphological characteristics of PBMCs-derived macrophages M1 (c) and M2 (d) in presence or not of recombinant spike. (e) Graphical representations of cell count. Values are expressed as rounded/stretched-dendritic ratio. The mean and standard deviation values were obtained from 6 independent experiments.

Macintosh. A p-value ≤0.05 was considered statistically significant. *P ≤ 0.05, **P < 0.01, ***P < 0.001, ****P < 0.0001.

3. Results

3.1. Spike induces morphological and functional M2 to M1 macrophage switch

We polarized peripheral blood monocytes into M1 or M2 macrophages. Successful polarization was assessed by qPCR according to the ARG/INOS ratio that, in the case of M1, was in favor of INOS (Fig. 1a) and vice versa for M2 (Fig. 1b). Then, macrophages were seeded onto plates precoated or not with recombinant spike (Fig. 1c and d). Typically, M1 macrophages appear rounded, flat, and amoeboid shaped (Fig. 1c, left); no significant changes in morphology were registered in the presence of spike (Fig. 1c, right). M2 macrophages are stretched with thin protrusions (Fig. 1d, left) [23] and tend to become round/slightly elongated in the presence of the spike (Fig. 1d, right). The counts of round/slightly elongated vs. stretched/dendritic forms showed that spike induced morphologic switch of M2 macrophages into M1 (Fig. 1e). Morphology of macrophages was unaffected in BSA-precoated monolayers (Fig. S1). PI positive cells (dead cells) were <5 %/field (range 0,6%-4,7 %) (Supplementary Fig. S2). To address whether the M1-like morphologic changes corresponded to an M1-gain of function, we investigated, in autologous coculture (CC) assay, whether the spike promoted the ability of M2 to stimulate an adaptive immune response. To this end, we performed cocultures of differentiated M1 and M2 macrophages with CD3-activated autologous PBMCs. Primary monocytes were polarized into M1 or M2 according to Yu et al. [18] and then incubated in the absence or the presence of recombinant spike. Differentiated macrophages were assessed by flow cytometry using the M1 marker CD80 and the M2 marker CD206. After placing a gate on live cells (Figs. S3a and b), expressions of CD80 and CD206 were measured (Fig. 2a and b; representative histograms in Fig. S3c). CD80 stained 62,1 % ± 1,5 of M1 and 13,6 % ± 2,3 of M2 (p < 0,0001)

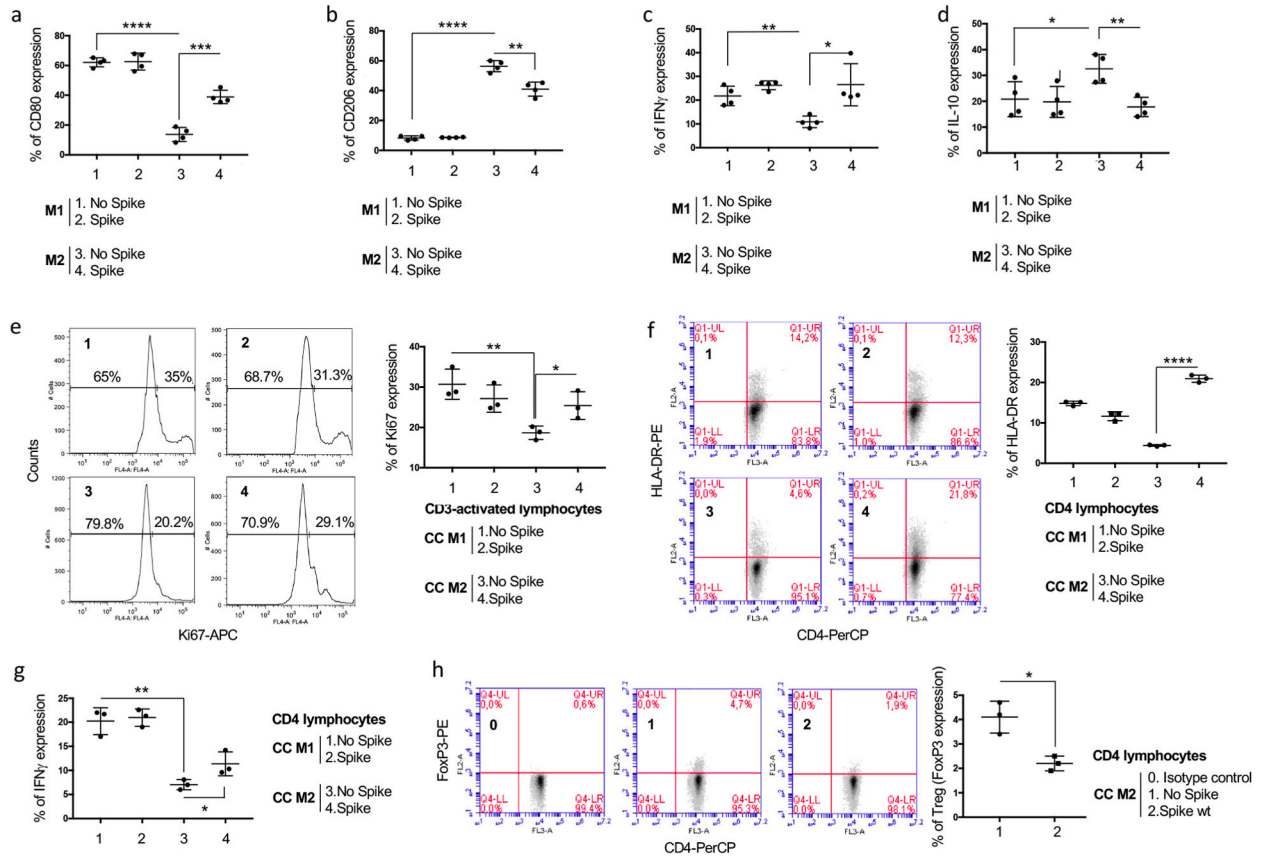

Fig. 2. Spike increases the M2 capability of inducing the adaptive immune response (a) Graphical representation of the values (%) of CD80 (a), CD206 (b), IFNγ (c), IL-10 (d) expression in M1 or M2 macrophages exposed or not to recombinant spike. (e) Measure of proliferation of activated CD3-T cells cocultured with autologous M1 or M2 macrophages in presence or not of recombinant spike. Ki67 was used as proliferation marker. Left, representative flow cytometry histograms of Ki67 expression in gated CD3 lymphocytes. Right, graphical representation of the values (%). (f) Measure of lymphocyte HLA-DR expression in CC lymphocytes. Representative flow cytometry histograms (left) and graphic representation (right) of values (%) of HLA-DR in activated CD4 lymphocytes in M1 or M2 macrophages CC, with or without spike. (g) Measure of lymphocyte IFNγ expression in CC lymphocytes. (h) Representative flow cytometry histograms (left) and graphic representation (right) of Treg count in CC with M2 macrophages, exposed or not to spike. The mean and standard deviation values were obtained from independent experiments (each point corresponds to a single experiment).

in the absence of spike, and 62,6 % ± 2,8 of M1 and 38,8 ± 2,2 of M2 in the presence of spike (n = 4) (Fig. 2a). CD80 expression on spike-treated M2 macrophages was significantly higher (p = 0,002) than expression on untreated M2 macrophages (Fig. 2a). CD206 stained 8,3 % ± 0,7 of M1 and 56,4 % ± 1,9 of M2 (p < 0,0001) in the absence of spike, and 8,6 % ± 0,1 of M1 and 40,9 ± 2,3 of M2 in the presence of spike (n = 4) (Fig. 2b). CD206 expression on spike-treated M2 macrophages was significantly lower (p = 0,02) than expression on untreated M2 macrophages (Fig. 2b). Intracellular levels of IFNγ and IL-10 (respectively M1 and M2 related cytokines) were in line with polarization (Fig. 2c and d, representative histograms in Fig. S3d). In CC, lymphocytes were gated according to CD4/SSC parameters (Fig. S4a). We assayed the proliferation of lymphocytes by flow cytometry after 72 h of CC, using the proliferation marker Ki67 (Fig. 2e). As expected, lymphocyte proliferation in M1 CC (Ki67 = 30,7 % ± 2,1; n = 3) was higher (p = 0,007) than that of M2 CC (Ki67 = 18,67 % ± 0,9; n = 3) (Fig. 2e). While the spike did not affect the costimulatory ability of M1 macrophages (Fig. 2e), a significant increase of lymphocyte proliferation (p = 0,02) was registered in CC with spike-stimulated M2 macrophages, compared to untreated M2 CC (Fig. 2e). To confirm the increased activation of lymphocytes, we measured HLA-DR expression on CD4 T lymphocytes (Fig. 2f) that was 4,4 % ± 0,12 and 20,9 % ± 0,5 in CC with untreated- or spike treated-M2 (p < 0,0001, n = 3). Measure of intracellular IFNγ in activated lymphocytes showed that 20.2 % ± 1.6 and 7.0 % ± 0.6 of lymphocytes expressed IFNγ (p = 0,002, n = 3) in CC with M1 and M2, respectively, while the values were 20,9 % ± 1,0 and 11,3 ± 1,4 in CC with spike-treated M1 or M2 macrophages, respectively (Fig. 2f, n = 3; representative histograms in Fig. S4b). IFNγ expression in lymphocytes from CC with spike-treated M2 macrophages was significantly lower (p = 0,049, n = 3) than that of lymphocytes from CC with untreated M2 macrophages (Fig. 2e). Moreover, a decrease in regulatory T cells (Tregs) was registered in spike-treated M2 CC (Fig. 2f). Treg counts were 4,1 % ± 0,3 and 2,2 % ± 0,1 in CC with untreated- or spike treated- M2 macrophages (p = 0,01; n = 3) (Fig. 2e).

3.2. Blockade of β3 integrin reverts the spike-induced costimulatory effects on M2 macrophages

We measured ACE2 and β3 integrin expression levels by flow cytometry on the plasma membrane of M1 and M2 macrophages (see Supplementary Fig. S5a for characterization). Fig. 3a shows expression levels of the two receptors in a biparametric flow cytometry dot plot. ACE2 was expressed in both macrophage subtypes at similar levels (n = 4) (Fig. 3a), while β3 integrin was present on the plasma membrane of M2 macrophages at a higher level (p = 0,01) than M1 macrophages (Fig. 3a). This result raised the hypothesis of a role for

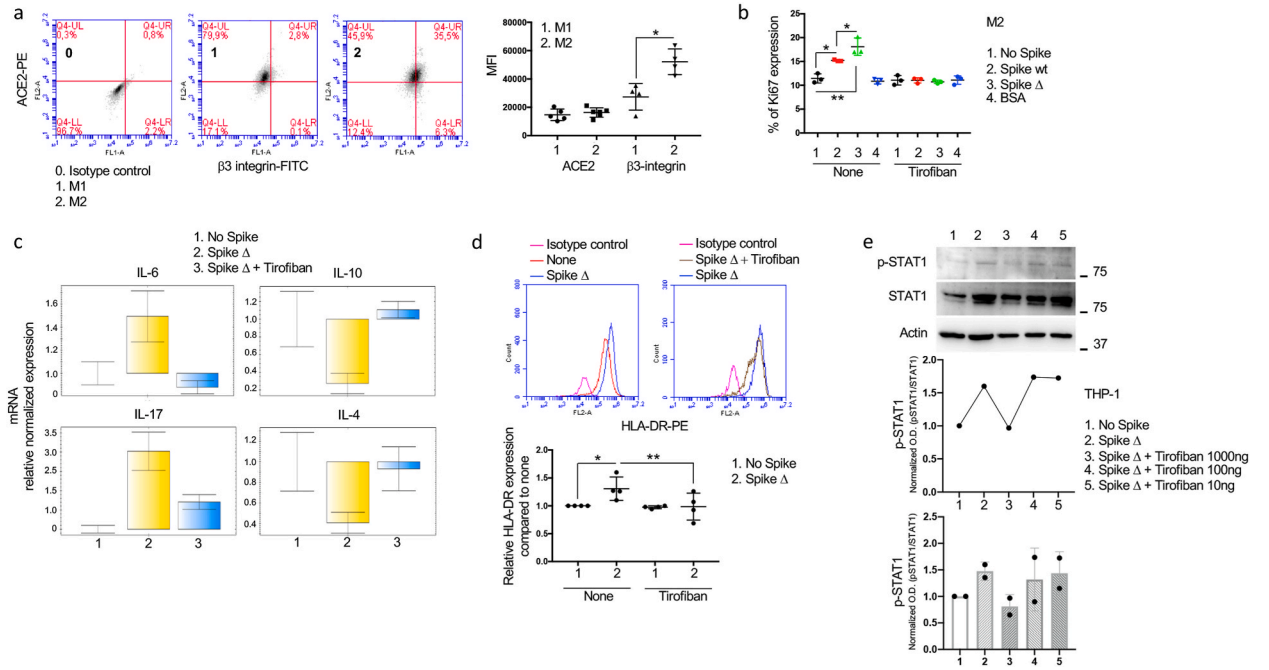

Fig. 3. Tirofiban prevents spike-induced M2 to M1 switch (a) Representative flow cytometry histograms (left) and graphical representation (right) of values (MFI) of ACE2 and β3 integrin in PBMCs-derived macrophages M1 and M2. (b) Graphical representation of the measure of lymphocyte proliferation using Ki67 proliferation marker. Activated PBMCs were cocultured with autologous M2 macrophages, exposed or not to recombinant spike wt, spikeΔ or BSA, in the presence or absence of 1 μg/ml tirofiban. The mean and standard deviation values were obtained from independent experiments (each point corresponds to a single experiment. (c) RT-qPCR analysis of mRNA levels of IL-6, IL-10, IL-17, IL-4 in PBMC-derived M2 macrophages exposed to spikeΔ in the presence or not of 1 μg/ml tirofiban. Values are expressed as mRNA relative normalized expression. (d) Representative flow cytometry histograms (top) and graphical representation (bottom) of values of HLA-DR expression on PBMC-derived M2 macrophage exposed to spikeΔ in the presence or not of 1 μg/ml tirofiban. (e) Immunoblot of the expression levels of p-STAT1 and STAT1 in THP1-derived M2 macrophages exposed to spikeΔ in the presence or not of tirofiban (1 μg/ml, 100 ng/ml, 10 ng/ml). β-Actin was used as loading control. Densitometric analysis of immunoblot is shown (raw image in Supplementary Material Fig. S9).

β3 integrin in M2 response to recombinant spike. To address this issue, we used tirofiban, a small molecule that selectively binds to β3 integrin with high affinity and investigated whether the spike effects were contrasted. Moreover, to verify the specificity of the spike effect, we used plates precoated with spikeΔ as positive control or BSA as negative control. M2 macrophage expression levels of CD80 and CD206 were modulated by spike wt and spike Δ. Precisely, they were increased and decreased, respectively, by spikes (Fig. S5b). Addition of tirofiban prevented such a modulation (Fig. S5b). Spike did not influence M1 macrophage expression of such markers (Fig. S5c). Then, to address whether tirofiban reverted the costimulatory effect of spike-treated M2 on lymphocyte proliferation, we performed lymphocyte CC with M2 macrophages, pretreated with spike wt or spikeΔ or BSA as control, in the absence or the presence of tirofiban (Fig. 3b). Measurement of the proliferation of cocultured lymphocytes showed that spikeΔ produced a costimulatory effect on M2 macrophages (Ki67 = 18,1 ± 1,8) higher (p = 0,005; n = 3) than that of untreated M2 (Ki67 = 11,4 ± 0,9) and even higher (p = 0,05; n = 3) than that induced by treatment with spike wt (Ki67 = 15,2 ± 0,17) (Fig. 3b) while BSA effect was neutral (Fig. 3b). The spike-costimulation effect was contrasted by tirofiban (Fig. 3b). QPCR of RNA extracted by M2 macrophages revealed that spikeΔ modulated transcript levels of the proinflammatory IL-17 and IL-6 and anti-inflammatory IL-4 and IL-10 cytokines that were prevented by tirofiban (Fig. 3c). SpikeΔ increased HLA-DR on M2 macrophages but not in the presence of tirofiban (Fig. 3d). The signal transducer and activator of transcription 1 (STAT1) is a pivotal mediator of M1 macrophage polarization and function. THP-1-derived M2, when stimulated with spikeΔ, showed activation of STAT1 that was prevented by the addition of tirofiban at the optimal dose of 1 μg/ml [17] but not at the lower doses of 100 and 10 ng/ml (Fig. 3e). Consistent with results with primary macrophages, Supplementary Fig. S6 shows that THP-1-derived-M1 and -M2 macrophages had similar ACE2 expression (Supplementary Fig. S6a) while M2 had higher β3 expression than M1-polarized THP-1 (Supplementary Fig. S6b). Interestingly, spike wt had a scarce effect on THP-1-polarized macrophages, as suggested by the finding that the costimulatory antigens HLA-DR and CD80 were upregulated on M2 macrophages stimulated by spikeΔ and not wt (Supplementary Fig. S6c). The spikes did not affect HLA-DR and CD80 expression on M1-THP-1 (Fig. S6d). Moreover, expression of active STAT1, a M1 hallmark, was not affected by spike stimulation (Supplementary Fig. S7). We then evaluated whether tirofiban promoted recovering the original M2 morphological form lost following the spike contact. As shown in Fig. 4a and b, in the presence of tirofiban, we could not observe the M1-like morphologic changes induced by spike wt spikeΔ on primary M2 macrophages.

3.3. Endothelial cells cultured with spike undergo apoptosis

In SARS-Cov-2 infection, activation of JAK/STAT1/IRF1 axis [24] has a detrimental effect on endothelial cell function and triggers inflammatory cell death. We investigated the impact of spike protein on STAT1 induction in the ECV cell line, a valuable model for studying cellular processes in the endothelium [25]. Western blot assay of ECV showed a marked effect of spike Δ on STAT1 activation (Fig. 5a) accompanied by increase in HLA-DR expression (Fig. 5b). Tirofiban reverted such spikeΔ-mediated effects (5a, b). Analysis of apoptosis performed on the primary endothelial cell line HUVEC showed that spikeΔ induced cell death that was contrasted when

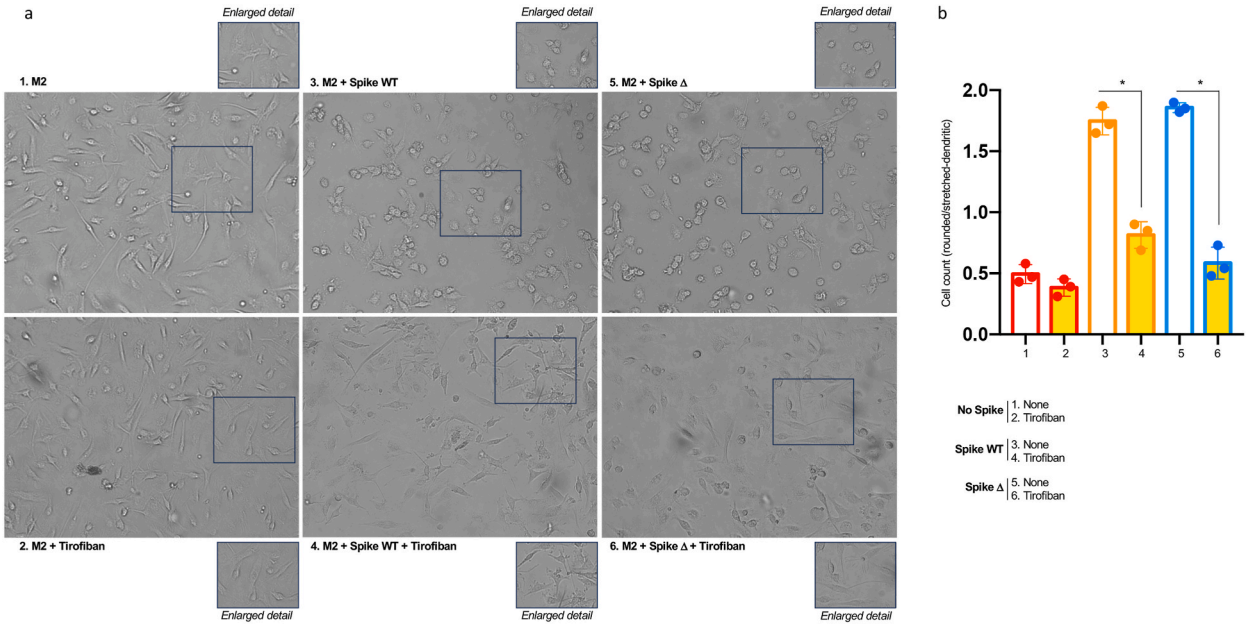

Fig. 4. Tirofiban counteracts spike-induced M2 to M1 morphologic switch (a) Representative images acquired under an inverted microscope (Leica DMI4000) at 20 × magnification showing morphological characteristics of PBMC-derived M2 macrophages exposed to spike wt or spikeΔ in the presence or not of 1 μg/ml tirofiban. (b) Graphical representations of cell count. Values are expressed as rounded/stretched-dendritic ratio. The mean and standard deviation values were obtained from 3 independent experiments.

tirofiban was added to the culture (Fig. 5c). A Western blot of protein extracted from spikeΔ-stimulated ECV showed that Bax upregulation accompanied STAT1 activation (Fig. 5d). The same blot shows that, like tirofiban, abcximab, a β3 integrin monoclonal antibody, contrasted the spikeΔ effects on STAT1 and Bax, (Fig. 5d). The expression level of a different STAT transcription factor, i.e., STAT3, did not appear to be affected by spikeΔ stimulation (Fig. 5d). Also, we could not appreciate any modulation of Bcl-2 expression levels following spike stimulation, alone or in the presence of β3-integrin inhibitors (Supplementary Fig. S8).

4. Discussion

Several authors have reported a direct role for spike protein in inducing the proinflammatory aspects of macrophages. Barhoumi et al. showed that stimulation of THP-1 macrophages with the spike protein upregulates the expression of TNF-α and MHC-II [26]. Mohammad et al. found that SARS-CoV-2 proteins induced concentration-dependent alterations in the metabolic and phenotypic profiles of macrophages in human monocyte-derived macrophages, possibly involved in the adverse effects of the disease [27]. Khan et al. showed that the spike protein triggers inflammation via activation of the NF-κB pathway and IL-6, TNF-α, and IL-1β mediated by stimulation of toll-like receptor 2 (TLR2) [28]. Dosh et al. also reported a role for spike protein in activating the NF-κB pathway in human monocyte/macrophages in vitro [29]. Palestra et al. involved the spike protein in activating the secretion of inflammatory chemokines and cytokines from primary human lung macrophages, independent of TLR2 [30].

Our study confirms that spike activates pro-inflammatory macrophages but adds a novel piece of information identifying M2 macrophages as the major spike-responsive cell subtype. We found that recombinant spike induced M1 morphological features in M2-polarized macrophages. Upon spike exposure, M2 macrophages lose their stretched/elongated/dendritic morphology, become almost rounded and their capability to stimulate lymphocyte activation and proliferation results in a significant increase.

We found that blockade of β3 integrin with the RGD mimetic tirofiban prevented the spike effect on M2 to M1 reprogramming. Unlike M1 macrophages, where integrin β3 levels were negligible, M2 macrophages expressed measurable levels of this receptor,

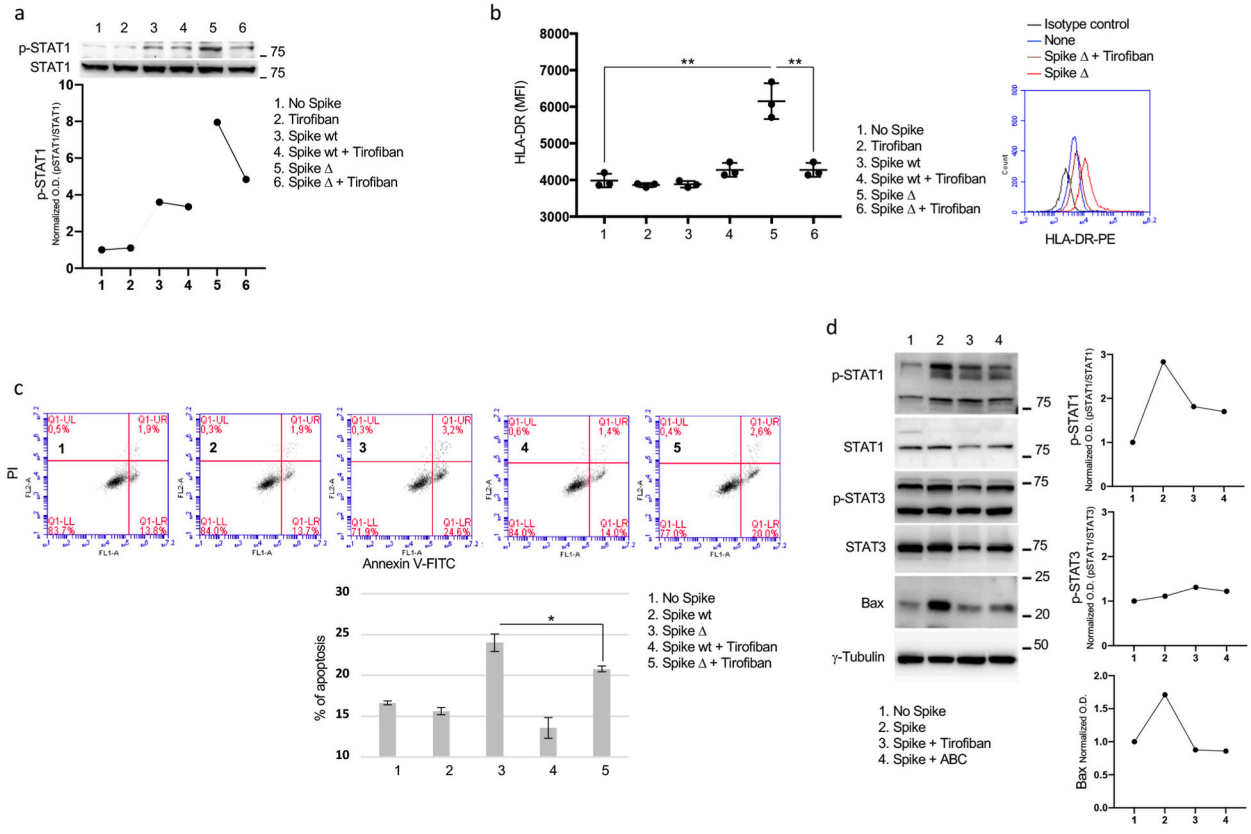

Fig. 5. Spike Δ induces STAT1 activation and promotes endothelial cell death (a) Immunoblot of the expression levels of p-STAT1 and STAT1 in ECV exposed to recombinant spike wt or spike Δ, in the presence or absence of 1 μg/ml tirofiban (top). Densitometric analysis of immunoblot is shown (raw image in Supplementary Material Fig. S10). (b) Graphical representation (top) and representative flow cytometry histograms (bottom) of values (mean fluorescence intensity, MFI) of HLA-DR expression on ECV exposed to recombinant spike wt or Δ, in the presence or not of 1 μg/ml tirofiban. (c) Representative flow cytometry histograms (top) and graphical representation (bottom) of apoptosis (annexin V-PI staining) in HUVEC exposed to recombinant spike wt or Δ, in the presence or not of 1 μg/ml tirofiban (n = 4). (d) Immunoblot of the expression levels of p-STAT1, STAT1 and BAX in ECV exposed to recombinant spike Δ, in the presence or not of 1 μg/ml tirofiban or 10 μg/ml abcximab. γ-Tubulin was used as loading control (left). Densitometric analysis of immunoblot is shown (raw image in Supplementary Material Fig. S11).

providing a possible explanation for the different responsiveness to the spike activating effect between the two cell subtypes. An increase of IL-6 was registered in spike-stimulated M2 macrophages, along with IL-17A, a cytokine that represses Treg induction [31], consistent with reduced counts of Tregs in spike-M2 CC. Parallely, the anti-inflammatory cytokine IL-4 and IL-10 levels were decreased. The signal transducer and activator-1 is pivotal for M1 polarization [13]: spike induced STAT1 activation in M2 macrophages, effectively contrasted by tirofiban.

Caccuri et al. showed that SARS-CoV-2 gains access into primary human lung microvascular endothelial cells lacking ACE2 expression through the conserved RGD motif [32]. Interestingly, the ECV cell line, a widely used endothelial cell model that is not susceptible to infection by SARS-Cov-2 [33], responded to spike Δ with STAT1 activation, prevented by β3 integrin blockade. Moreover, in accordance with Karki et al. [24] that in SARS-Cov-2 infection, activation of JAK/STAT1/IRF1 axis triggers inflammatory cell death, we found Bax upregulation accompanying STAT1 activation in ECV stimulated with spike Δ and registered endothelial cell apoptosis. Overall, these effects were prevented by β3 integrin blockade.

Our study has some limitations; first, we investigated the spike effect on the M2 subset classically induced by IL-4, despite the existence of a range of M2 subtypes. Secondly, among the many variants of the spike protein, some of which are very virulent, only two have been considered. However, it should be emphasized that, with its limitations, our study identifies a new role for the spike protein, namely M2 to M1 macrophage reprogramming, which could be involved in the reactivation of inflammation when the disease appears to be resolving. Our study could have implications for the safe development of protein-based vaccines and open the door for RGD mimetics as new drugs against SARS-Cov-2.

Financial support

This work was funded by Unione Europea-NextGenerationEU Project Code: PNRR-MR1-2022-12376524.

Funding

PRIN 2022 - Progetti di Rilevante Interesse Nazionale funded by MUR (Project code: 20222N3X8L).

Data availability statement

All data are available in the article, in the supplemental material, or in a public open access repository (https://github.com/MMBMrepository/HELIYON-D-23-35780.git).

Ethics declarations

The Federico II University Ethics Committee approved these research experiments (protocol n. 12/11/ES19) that were conducted in accordance with the ethical principles of the Declaration of Helsinki. Informed consent was obtained from all blood donor providers of PBMCs.

CRediT authorship contribution statement

Laura Marrone: Methodology, Formal analysis, Data curation. **Simona Romano:** Writing – review & editing, Methodology, Formal analysis, Data curation. **Michele Albanese:** Formal analysis, Data curation. **Salvatore Giordano:** Formal analysis, Data curation. **Alberto Morello:** Formal analysis, Data curation. **Michele Cimmino:** Formal analysis, Data curation. **Valeria Di Giacomo:** Methodology. **Chiara Malasomma:** Methodology, Formal analysis, Data curation. **Maria Fiammetta Romano:** Writing – review & editing, Writing – original draft, Supervision, Formal analysis, Data curation, Conceptualization. **Nicola Corcione:** Writing – original draft, Supervision, Data curation, Conceptualization.

Declaration of competing interest

The authors declare that they have no known competing financial interests or personal relationships that could have appeared to influence the work reported in this paper.

Acknowledgments

We thank Cardiovascular Service S. r.l. For supporting our study.

Appendix A. Supplementary data

Supplementary data to this article can be found online at https://doi.org/10.1016/j.heliyon.2024.e35341.

References

[1] I. Hamming, W. Timens, M.L. Bulthuis, A.T. Lely, G. Navis, H. van Goor, Tissue distribution of ACE2 protein, the functional receptor for SARS coronavirus. A first step in understanding SARS pathogenesis, J. Pathol. 203 (2) (2004 Jun) 631–637, https://doi.org/10.1002/path.1570.

[2] M. Donoghue, F. Hsieh, E. Baronas, K. Godbout, M. Gosselin, N. Stagliano, M. Donovan, B. Woolf, K. Robison, R. Jeyaseelan, R.E. Breitbart, S. Acton, A novel angiotensin-converting enzyme-related carboxypeptidase (ACE2) converts angiotensin I to angiotensin 1-9, Circ. Res. 87 (5) (2000 Sep 1) E1–E9, https://doi.org/10.1161/01.res.87.5.e1.

[3] J. Kliche, H. Kuss, M. Ali, Y. Ivarsson, Cytoplasmic short linear motifs in ACE2 and integrin β_3 link SARS-CoV-2 host cell receptors to mediators of endocytosis and autophagy, Sci. Signal. 14 (665) (2021 Jan 12) eabf1117, https://doi.org/10.1126/scisignal.abf1117.

[4] A. Bugatti, F. Filippini, M. Bardelli, A. Zani, P. Chiodelli, S. Messali, A. Caruso, F. Caccuri, SARS-CoV-2 infects human ACE2-negative endothelial cells through an $\alpha_v\beta_3$ integrin-mediated endocytosis even in the presence of vaccine-elicited neutralizing antibodies, Viruses 14 (4) (2022 Mar 29) 705, https://doi.org/10.3390/v14040705.

[5] C.J. Sigrist, A. Bridge, P. Le Mercier, A potential role for integrins in host cell entry by SARS-CoV-2, Antivir. Res. 177 (2020 May) 104759, https://doi.org/10.1016/j.antiviral.2020.104759.

[6] M. Soy, G. Keser, P. Atagündüz, F. Tabak, I. Atagündüz, S. Kayhan, Cytokine storm in COVID-19: pathogenesis and overview of anti-inflammatory agents used in treatment, Clin. Rheumatol. 39 (7) (2020 Jul) 2085–2094, https://doi.org/10.1007/s10067-020-05190-5.

[7] P. Mehta, D.F. McAuley, M. Brown, E. Sanchez, R.S. Tattersall, J.J. Manson, COVID-19: consider cytokine storm syndromes and immunosuppression, Lancet 395 (2020) 1033–1034, https://doi.org/10.1016/S0140-6736(20)30628-0.

[8] C. Blériot, S. Chakarov, F. Ginhoux, Determinants of resident tissue macrophage identity and function, Immunity 52 (6) (2020 Jun 16) 957–970, https://doi.org/10.1016/j.immuni.2020.05.014.

[9] F.O. Martinez, A. Sica, A. Mantovani, M. Locati, Macrophage activation and polarization, Front. Biosci. 13 (2008 Jan 1) 453–461, https://doi.org/10.2741/2692.

[10] P.J. Murray, J.E. Allen, S.K. Biswas, E.A. Fisher, D.W. Gilroy, S. Goerdt, S. Gordon, J.A. Hamilton, L.B. Ivashkiv, T. Lawrence, M. Locati, A. Mantovani, F. O. Martinez, J.L. Mege, D.M. Mosser, G. Natoli, J.P. Saeij, J.L. Schultze, K.A. Shirey, A. Sica, J. Suttles, I. Udalova, J.A. van Ginderachter, S.N. Vogel, T.A. Wynn, Macrophage activation and polarization: nomenclature and experimental guidelines, Immunity 41 (1) (2014 Jul 17) 14–20, https://doi.org/10.1016/j.immuni.2014.06.008.

[11] S. Gordon, F.O. Martinez, Alternative activation of macrophages: mechanism and functions, Immunity 32 (5) (2010 May 28) 593–604, https://doi.org/10.1016/j.immuni.2010.05.007.

[12] P. Italiani, D. Boraschi, From monocytes to M1/M2 macrophages: phenotypical vs. Functional differentiation, Front. Immunol. 5 (2014 Oct 17) 514, https://doi.org/10.3389/fimmu.2014.00514.

[13] Y. Yao, X.H. Xu, L. Jin, Macrophage polarization in physiological and pathological pregnancy, Front. Immunol. 10 (2019 Apr 15) 792, https://doi.org/10.3389/fimmu.2019.00792.

[14] J. Sapudom, S. Karaman, W.K.E. Mohamed, A. Garcia-Sabaté, B.C. Quartey, J.C.M. Teo, 3D in vitro M2 macrophage model to mimic modulation of tissue repair, NPJ Regen Med 6 (1) (2021 Nov 30) 83, https://doi.org/10.1038/s41536-021-00193-5.

[15] P.J. Murray, Macrophage polarization, Annu. Rev. Physiol. 79 (2017 Feb 10) 541–566, https://doi.org/10.1146/annurev-physiol-022516-034339.

[16] H.E. Davis, L. McCorkell, J.M. Vogel, E.J. Topol, Long COVID: major findings, mechanisms and recommendations, Nat. Rev. Microbiol. 21 (3) (2023 Mar) 133–146, https://doi.org/10.1038/s41579-022-00846-2.

[17] A. Giordano, A. D'Angelillo, S. Romano, P. D'Arrigo, N. Corcione, R. Bisogni, S. Messina, M. Polimeno, P. Pepino, P. Ferraro, M.F. Romano, Tirofiban induces VEGF production and stimulates migration and proliferation of endothelial cells, Vasc. Pharmacol. 61 (2–3) (2014 May-Jun) 63–71, https://doi.org/10.1016/j.vph.2014.04.002.

[18] T. Yu, S. Gan, Q. Zhu, D. Dai, N. Li, H. Wang, X. Chen, D. Hou, Y. Wang, Q. Pan, J. Xu, X. Zhang, J. Liu, S. Pei, C. Peng, P. Wu, S. Romano, C. Mao, M. Huang, X. Zhu, K. Shen, J. Qin, Y. Xiao, Modulation of M2 macrophage polarization by the crosstalk between Stat6 and Trim24, Nat. Commun. 10 (1) (2019 Sep 25) 4353, https://doi.org/10.1038/s41467-019-12384-2.

[19] E.W. Baxter, A.E. Graham, N.A. Re, I.M. Carr, J.I. Robinson, S.L. Mackie, A.W. Morgan, Standardized protocols for differentiation of THP-1 cells to macrophages with distinct M(IFNγ+LPS), M(IL-4) and M(IL-10) phenotypes, J. Immunol. Methods 478 (2020 Mar) 112721, https://doi.org/10.1016/j.jim.2019.112721.

[20] T. Troiani, E.F. Giunta, M. Tufano, V. Vigorito, P. Arrigo, G. Argenziano, F. Ciardiello, M.F. Romano, S. Romano, Alternative macrophage polarisation associated with resistance to anti-PD1 blockade is possibly supported by the splicing of FKBP51 immunophilin in melanoma patients, Br. J. Cancer 122 (12) (2020 Jun) 1782–1790, https://doi.org/10.1038/s41416-020-0840-8.

[21] D. Russo, F. Merolla, M. Mascolo, G. Ilardi, S. Romano, S. Varricchio, V. Napolitano, A. Celetti, L. Postiglione, P.P. Di Lorenzo, L. Califano, G.O. Dell'Aversana, F. Astarita, M.F. Romano, S. Staibano, FKBP51 immunohistochemical expression: a new prognostic biomarker for OSCC? Int. J. Mol. Sci. 18 (2) (2017 Feb 18) 443, https://doi.org/10.3390/ijms18020443.

[22] S. Romano, M. Mallardo, F. Chiurazzi, R. Bisogni, A. D'Angelillo, R. Liuzzi, G. Compare, M.F. Romano, The effect of FK506 on transforming growth factor beta signaling and apoptosis in chronic lymphocytic leukemia B cells, Haematologica 93 (7) (2008 Jul) 1039–1048, https://doi.org/10.3324/haematol.12402.

[23] H.M. Rostam, P.M. Reynolds, M.R. Alexander, N. Gadegaard, A.M. Ghaemmaghami, Image based Machine Learning for identification of macrophage subsets, Sci. Rep. 7 (1) (2017 Jun 14) 3521, https://doi.org/10.1038/s41598-017-03780-z.

[24] R. Karki, B.R. Sharma, S. Tuladhar, E.P. Williams, L. Zalduondo, P. Samir, M. Zheng, B. Sundaram, B. Banoth, R.K.S. Malireddi, P. Schreiner, G. Neale, P. Vogel, R. Webby, C.B. Jonsson, T.D. Kanneganti, Synergism of TNF-α and IFN-γ triggers inflammatory cell death, tissue damage, and mortality in SARS-CoV-2 infection and cytokine shock syndromes, Cell 184 (1) (2021 Jan 7) 149–168.e17, https://doi.org/10.1016/j.cell.2020.11.025.

[25] W.C. Xiong, S. Simon, ECV304 cells: an endothelial or epithelial model? J. Biol. Chem. 286 (41) (2011 Oct 14) le21 https://doi.org/10.1074/jbc.N111.261073.

[26] T. Barhoumi, B. Alghanem, H. Shaibah, F.A. Mansour, H.S. Alamri, M.A. Akiel, F. Alroqi, M. Boudjelal, SARS-CoV-2 coronavirus spike protein-induced apoptosis, inflammatory, and oxidative stress responses in THP-1-like-macrophages: potential role of angiotensin-converting enzyme inhibitor (perindopril), Front. Immunol. 12 (2021 Sep 20) 728896, https://doi.org/10.3389/fimmu.2021.728896.

[27] M.G. Mohammad, N.S. Ashmawy, A.M. Al-Rawi, A. Abu-Qiyas, A.M. Hamoda, R. Hamdy, S. Dakalbab, S. Arikat, D. Salahat, M. Madkour, S.S.M. Soliman, SARS-CoV-2-free residual proteins mediated phenotypic and metabolic changes in peripheral blood monocytic-derived macrophages in support of viral pathogenesis, PLoS One 18 (1) (2023 Jan 19) e0280592, https://doi.org/10.1371/journal.pone.0280592.

[28] S. Khan, M.S. Shafiei, C. Longoria, J.W. Schoggins, R.C. Savani, H. Zaki, SARS-CoV-2 spike protein induces inflammation via TLR2-dependent activation of the NF-κB pathway, Elife 10 (2021 Dec 6) e68563, https://doi.org/10.7554/eLife.68563.

[29] S.F. Dosch, S.D. Mahajan, A.R. Collins, SARS coronavirus spike protein-induced innate immune response occurs via activation of the NF-kappaB pathway in human monocyte macrophages in vitro, Virus Res. 142 (1–2) (2009 Jun) 19–27, https://doi.org/10.1016/j.virusres.2009.01.005.

[30] F. Palestra, R. Poto, R. Ciardi, G. Opromolla, A. Secondo, V. Tedeschi, A.L. Ferrara, R.M. Di Crescenzo, M.R. Galdiero, L. Cristinziano, L. Modestino, G. Marone, A. Fiorelli, G. Varricchi, S. Loffredo, SARS-CoV-2 spike protein activates human lung macrophages, Int. J. Mol. Sci. 24 (3) (2023 Feb 3) 3036, https://doi.org/10.3390/ijms24033036.

[31] R. Thomas, S. Qiao, X. Yang, Th17/Treg imbalance: implications in lung inflammatory diseases, Int. J. Mol. Sci. 24 (5) (2023 Mar 2) 4865, https://doi.org/10.3390/ijms24054865.

[32] F. Caccuri, A. Bugatti, A. Zani, A. De Palma, D. Di Silvestre, E. Manocha, F. Filippini, S. Messali, P. Chiodelli, G. Campisi, S. Fiorentini, F. Facchetti, P. Mauri, A. Caruso, SARS-CoV-2 infection remodels the phenotype and promotes angiogenesis of primary human lung endothelial cells, Microorganisms 9 (7) (2021 Jul 3) 1438, https://doi.org/10.3390/microorganisms9071438.

[33] N. Wurtz, G. Penant, P. Jardot, N. Duclos, B. La Scola, Culture of SARS-CoV-2 in a panel of laboratory cell lines, permissivity, and differences in growth profile, Eur. J. Clin. Microbiol. Infect. Dis. 40 (3) (2021 Mar) 477–484, https://doi.org/10.1007/s10096-020-04106-0.